Analytic optical-constant model derived from Tauc-Lorentz and Urbach tail

LUIS V. RODRÍGUEZ-DE MARCOS,[1,2] JUAN I. LARRUQUERT[1,*]

[1]*GOLD-Instituto de Óptica-Consejo Superior de Investigaciones Científicas*
Serrano 144, 28006 Madrid, Spain
[2]*lv.rodriguez@io.cfmac.csic.es*
**j.larruquert@csic.es*

Abstract: Tauc-Lorentz model is commonly used to describe the dielectric constant of amorphous semiconductors as a function of few parameters. However, this model is not fully analytic and presents other mathematical shortcomings. A modified self-consistent model based on the integration of [E'-(E+ia)]-1 functions using Tauc-Lorentz`s ε_2 expression as a weight function is presented. This new model is analytic and meets all other mathematical requirements of optical constants. The main difference with TL model stands at photon energies close to or smaller than the bandgap energy.

The new model has been satisfactorily tested on SiC optical constants. Additionally, an analytic extension of the new model has been also developed to include the Urbach tail. The complete model has been tested with Si_3N_4 optical constants, and it enables to extend the optical-constant characterization of materials down to zero energy.

OCIS codes: (120.4530) Optical constants; (310.6860) Thin films, optical properties; (160.6000) Semiconductor materials; (300.6470) Spectroscopy, semiconductors; (120.2130) Ellipsometry and polarimetry.

References and links

1. A. R. Forouhi and I. Bloomer, "Optical dispersion relations for amorphous semiconductors and amorphous dielectric," Phys. Rev. B **34**, 7018-7026 (1986).
2. D. Campi and C. Coriasso, "Prediction of optical properties of amorphous tetrahedrally bonded materials," J. Appl. Phys. **64**, 4128-4134 (1988).
3. G. E. Jellison and F. A. Modine, "Parameterization of the optical functions of amorphous materials in the interband region," Appl. Phys. Lett., **69**, 371-373 (1996).
4. G. D. Cody, in J. I. Pankove (Ed.), *Semiconductors and Semimetals* vol. 21, p. 11 (Academic, 1984).
5. D. Franta, D. Nečas, I. Ohlidal, and A. Giglia, "Dispersion model for optical thin films applicable in wide spectral range," Proc. of SPIE **9628**, 96281U (2015).
6. M. Foldyna, K. Postava, J. Bouchala, J. Pitora, and T. Yamaguchi, "Model dielectric function of amorphous materials including Urbach tail," Proc. of SPIE **5445**, 301-305 (2003).
7. A. S. Ferlauto, J. Koh, P. I. Rovira, C. R. Wronski, R. W. Collins, and G. Ganguly, "Modeling the dielectric functions of silicon-based films in the amorphous, nanocrystalline and microcrystalline regimes," J. Non-Cryst. Solids **266**–269, 269-273 (2000).
8. J. I. Larruquert and L. V. Rodríguez-de Marcos, Instituto de Optica-CSIC, Serrano 144, Madrid 28006 Spain, are preparing a manuscript to be called "Procedure to convert optical-constant models into analytic."
9. J. Tauc, R. Grigorovici, and A. Vancu, "Optical properties and electronic structure of amorphous germanium," Phys. Stat. Sol. **15**, 627-637 (1966).
10. B. von Blanckenhagen, D. Tonova, and J. Ullmann, "Application of the Tauc–Lorentz formulation to the interband absorption of optical coating materials," Appl. Opt. **41**, 3137-3141 (2002).
11. R. Brendel and D. Bormann, "An infrared dielectric function model for amorphous solids," J. Appl. Phys. **71**, 1-6 (1992).
12. J. I. Larruquert, A. P. Pérez-Marín, S. García-Cortés, L. Rodríguez-de Marcos, J. A. Aznárez, and J. A. Méndez, "Self-consistent optical constants of SiC thin films," J. Opt. Soc. Am. A **28**, 2340-2345 (2011).
13. M. Abramowitz and I. Stegun, *Handbook of Mathematical Functions* (Dover Publications Inc., 1965).
14. V. Pegoraro and P. Slusallek, "On the evaluation of the complex-valued exponential integral," J. of Graphics, GPU, and Game Tools **15**, 183-198 (2011)
15. H. R. Philipp, "Optical Properties of Silicon Nitride," J. Electrochem. Soc. **120**, 295-300 (1973).
16. H. R. Philipp, "Silicon Nitride (Si3N4) (Noncrystalline)," in *Handbook of Optical Constants of Solids* D. Palik ed. (Academic Press, 1991).

1. Introduction

The optical constants of materials are necessary for different applications, such as the design, characterization and/or process control of coatings for optics or for the semiconductor industry. The optical properties of materials require the knowledge of two optical constants, such as n and k or ε_1 and ε_2, per photon energy. Often, such amount of information is not available. The optical properties of various groups of materials in nature have common features; this allows the use of simple models to describe their optical constants in certain spectral ranges, which depend on few parameters to be determined for each material. Semiconductors is a group of materials for which various models have been developed to parameterize their optical constants, such as the models of Forouhi and Bloomer [1] (FB), Campi and Coriasso [2], Tauc-Lorentz [3] (TL), or Cody-Lorentz [4]. If we broaden the scope of materials and the spectral range, the model will need more parameters to fit. This is the case for a recent model developed by Franta *et al.* [5], which is aimed to cover a broad spectral range and hence it depends on a large number of parameters.

Optical constants of materials must satisfy some requirements that arise from fundamental properties of the interaction of radiation with matter, such as causality and linearity. Hence causality results in that the optical constants of a material as a function of photon energy can be extended with an analytic function to complex energies in the upper half plane, with a given parity and with a fast enough decay towards large energies. All these properties are required to enable the Kramers-Kronig (KK) analysis, which connects the imaginary with the real part of the optical constant complex function, and vice-versa. One common problem of the aforementioned optical-constant models for semiconductors is that they are defined with piecewise functions with a change in the functional behaviour at the semiconductor gap and hence they are not analytic; an exception to this is FB, although this model does not work below the bandgap energy. Furthermore, among the mentioned models there are also cases of divergences, and parity violations.

In TL model the imaginary part of the dielectric constant ε_2 turns zero below the material bandgap energy, whereas in practice, semiconductors and dielectrics are known to experience an exponential decay of the absorption coefficient, α, below the bandgap, which is called the Urbach tail. Valuable models were proposed to incorporate the Urbach tail to the TL model by Foldyna *et al.* [6] and a similar extension to the Cody-Lorentz model was performed by Ferlauto *et al.* [7]. However, the corrected models keep the use of piecewise functions, so that the lack of analyticity is not solved.

The present paper focuses in TL, which is a popular model that is widely used in the literature. A separate paper [8] proposes a procedure to take optical constant models that are not fully analytic and transform them into analytic and self-consistent models. The procedure consists of using either the dispersion or the absorption term of the non-analytic model as a weight function of $[E'-(E+ia)]^{-1}$ functions that are integrated over their full spectral domain. This can be applied to several of the above models. The present paper is devoted to apply this procedure to transform the TL model into analytic; the new model is later modified to include the Urbach tail.

The paper is organized as follows. Section 2 describes the TL model and the aforementioned procedure to turn non-analytic models into analytic. In section 3, the standard TL model is transformed into analytic and both models are used to fit the optical constants of SiC films. Then the Urbach tail is added to the model, which is exemplified by fitting the optical constants of Si_3N_4.

2 Modification of an optical-constant model to make it analytic

2.1 The TL model

In this section we start mentioning the FB model and its shortcomings that TL model attempted to solve. We show that, in spite of that attempt, TL model still involves some shortcomings and we modify it to remove them.

Forouhi and Bloomer [1] published a model to describe the extinction coefficient *k* of amorphous semiconductors and insulators, assuming that both valence and conduction bands can be described by a parabolic function. The expression obtained for *n* and *k* was:

$$k_{FB} = \frac{A\left(E - E_g\right)^2}{E^2 - BE + C} \tag{1a}$$

$$n_{FB} = n_\infty + \frac{B_0 E + C_0}{E^2 - BE + C} \tag{1b}$$

where A, B, C, the energy gap E_g, and n_∞ are fitting parameters; B_0 and C_0 are parameters depending on the previous ones.

Jellison and Modine [3] highlighted the inconsistencies of the FB model. First, *k* in FB model does not tend to 0 both below E_g and at large energies. Second, *k* should be an odd function of energy but it is not. A new model was proposed by Jellison and Modine that is referred to as the Tauc-Lorentz model [3] since it combines Tauc's model of the density of states with the Lorentz oscillator. It starts with the work of Tauc *et al.* [9], who interpreted the presence of a gap in amorphous semiconductors as the energy of transitions without momentum conservation between extended states of the valence and conduction bands, assuming a parabolic behaviour of these bands and constant matrix elements of the momentum operator. TL model combines Tauc's density of states [8] along with the Lorentz oscillator, and is given by:

$$\varepsilon_{2,TL}\left(E; A, E_0, E_g, C\right) = \Theta\left(E - E_g\right)\frac{\left(E - E_g\right)^2 A E_0 C}{\left(E^2 - E_0^2\right)^2 + C^2 E^2}\cdot\frac{1}{E} \tag{2a}$$

where E_0 is the central energy of the oscillator, C is the oscillator width and A is a fitting parameter. Θ stands for the Heaviside function and it is +1 or 0 for photon energies above or below E_g, respectively; hence ε_2 is zero in TL model for energies below E_g. The following notation will be used with the dielectric function: the first term within parenthesis is the variable, and the terms separated by semicolon from the variable are fitting parameters of the model. This model uses four fitting parameters to model ε_2, all expressed in energy units. TL model obtains $\varepsilon_1$with KK analysis:

$$\varepsilon_{1,TL}\left(E; A, E_0, E_g, C, \varepsilon_1(\infty)\right) = \varepsilon_1(\infty) + \frac{2}{\pi}\int_{E_g}^{\infty}\frac{\varepsilon_{2,TL}\left(E'\right)E'}{E'^2 - E^2}dE' \tag{2b}$$

However, the model required the addition of a supplementary fitting parameter, $\varepsilon_1(\infty)$. For shortness, we do not copy the expression obtained upon integration of the right term of Eq. (2b); it can be found in [3].

TL model is nowadays among the most widely used optical-constant models to determine the dielectric constant of amorphous semiconductors above their gap energy and to determine the material bandgap energy [10]; the model is a standard element in many software packages for analyzing experimental measurements, particularly for ellipsometry measurements.

Even though TL model was an attempt to construct a mathematically correct and physically plausible model, a series of shortcomings have been detected. These shortcomings arise from not fully complying the conditions required for KK dispersion relations:

a) The dielectric constant is not analytic. A function that is analytic at a point must be infinitely differentiable in the neighbourhood of that point. Hence, ε_2 is not analytic in $E = E_g$. More generally, any piecewise function, such as Heaviside function, is not analytic at the connection point between two different functionalities. Furthermore, in TL model it is $\varepsilon_2=0$ in a finite range between E=0 and $E=E_g$, and the only analytic function to satisfy this is the null function, which obviously would not work here at $E>E_g$. Actually, experimental data of absorption in amorphous materials show that, even though absorption is small below the bandgap, it takes nonzero values. Due to the mentioned lack of analyticity, there is no possible analytic continuation of ε_2 in the upper complex half plane.
b) Parity: ε_2 is not odd due to the $(E-E_g)^2$ term, although this problem was avoided by defining ε_2 with opposite sign at negative energies.
c) The term $\varepsilon_1(\infty)$ was added to the model to improve the fitting, but this makes inconsistent the expression for ε_1, since ε_1 and ε_2 should be directly related through the KK analysis with no extra term.

Summarizing, though TL model was developed to correct inconsistencies of the FB model and it is usually taken as mathematically correct, it still has several shortcomings. TL model is currently one of the most popular models to fit the dielectric constant of amorphous semiconductor materials. However, it will be demonstrated in the following section that the new model fits experimental data more precisely at energies close to or below E_g.

2.2 Procedure to obtain an analytic model for optical constants out of a non-analytic model.

A mechanism to turn non-analytic optical-constant models into analytic has been recently developed [8]. Here we summarize the main equations for this, and in subsection 3.1 the procedure will be applied to the TL model. The mechanism operates by using either the real or the imaginary part of an optical-constant model, from either the complex refractive index or the complex dielectric constant, as a real weight function of $[E'-(E+ia)]^{-1}$ complex functions, which are integrated over the weight function full spectrum domain; E' stands for the integration energy parameter, E is the energy at which the optical constants are calculated, and $a>0$ is an added damping parameter. Hence the original optical-constant function is convolved with $[E'-(E+ia)]^{-1}$ functions, which results in some curve smoothening of the part used as weight function due to $a\neq 0$; this smoothening can be made as small as necessary by reducing a, so that the resulting analytic function is as close as desired to, but never fully coincident with, the original non-analytic function. In the following we reproduce one of the possible expressions of Larruquert and Rodríguez de Marcos in [8] to construct the analytic model using either the imaginary part [Eq. (3a)] or the real part [Eq. (3b)] of the non-analytic model:

$$\widetilde{\varepsilon}_{an}(E)-1=\frac{1}{\pi}\int_{-\infty}^{\infty}\frac{\varepsilon_{2,\mathrm{mod}}(E')}{E'-E-ia}dE' \tag{3a}$$

$$\widetilde{\varepsilon}_{an}(E)-1=-\frac{i}{\pi}\int_{-\infty}^{\infty}\frac{\varepsilon_{1,\mathrm{mod}}(E')-1}{E'-E-ia}dE' \tag{3b}$$

Eq. (3a) [(3b)] uses the imaginary part of the dielectric constant $\varepsilon_{2,\mathrm{mod}}$ (the real part $\varepsilon_{1,\mathrm{mod}}$) of the original model to construct an analytic optical-constant function $\widetilde{\varepsilon}_{an}(E)$. When a is small enough compared to the characteristic parameters of a certain material, the imaginary (or real) part of the dielectric constant of the analyticized model is very close to the same part of the original non-analytic model. In a specific case, we select either Eq. (3a) or (3b) depending on the part of the dielectric constant that we decide to use as a weight function. Equations (3) are valid for dielectrics or semiconductors, whereas for metals, Eqs. (3) must be slightly modified.

One benefit of using the mechanism given in in Eqs. (3) is that we can use a piecewise weight function for either $\varepsilon_{2,\mathrm{mod}}$ or $\varepsilon_{1,\mathrm{mod}}$-1, and the present procedure will turn the original non-analytic model into analytic. Analyticity in the complex upper half plane is given by the $[E'-(E+ia)]^{-1}$ terms, and the corresponding part of the dielectric constant purely operates as a real weight factor. As a result of this, the dielectric constant is somewhat smoothened, which results in an optical constant averaged mostly in the $E\pm a$ range. Since a can be made as small as necessary (but not zero) for a specific case, this smoothening may be made almost negligible.

The integrals in Eqs. (3) involve the superposition of $[E'-(E+ia)]^{-1}$ functions; these integrals satisfy the analyticity requirement. All other requirements to meet the criteria for KK analysis can be obtained too. The correct parity is provided by the $[E'-(E+ia)]^{-1}$ functions along with the assumed odd (even) functionality for $\varepsilon_{2,\mathrm{mod}}$ ($\varepsilon_{1,\mathrm{mod}}$). A fast enough asymptotic decay at $E\rightarrow\infty$ is obtained as long as the weight function also decays fast enough in that limit, which is satisfied by ε_2 for instance in the TL model.

The present procedure of constructing a dielectric function by convolving a desired profile with an analytic function has a precedent in the work of Brendel and Bormann [11]. In that research the analytic functions were Lorentz oscillators, and the real weight function was a Gaussian function.

3 Application to Tauc-Lorentz model

3.1 Analytic modification of Tauc-Lorentz model

Since TL model is developed over ε_2, we select the expression given by Eq. (2a) in the integration of Eq. (3a):

$$\widetilde{\varepsilon}_{TL-an}\left(E;A,E_0,E_g,C,a\right)=1+\frac{1}{\pi}\int_{-\infty}^{\infty}\frac{\varepsilon_{2,TL}\left(E'\right)}{E'-E-ia}dE' \tag{4}$$

where the sign of $\varepsilon_{2,\mathrm{Tl}}$ in expression (2a) was reversed for negative energies to turn it into an odd function.

Eq. (4) can be integrated and results in:

$$\widetilde{\varepsilon}_{TL-an}\left(E;A,E_0,E_g,C,a\right)=1+\frac{AE_0C}{\pi}\left[F\left(b,d,d^*\right)+F\left(d,d^*,b\right)+F\left(d^*,b,d\right)\right] \tag{5}$$

with:

$$F\left(\alpha,\beta,\gamma\right)=\frac{\left(E_g+\alpha\right)^2Log\left(E_g+\alpha\right)-\left(E_g-\alpha\right)^2Log\left(E_g-\alpha\right)}{\alpha\left(\alpha^2-\beta^2\right)\left(\alpha^2-\gamma^2\right)} \tag{6}$$

$$b\equiv b\left(E\right)=E+ia \tag{7}$$

$$d=\sqrt{E_0^2-\left(\frac{C}{2}\right)^2}-i\frac{C}{2} \tag{8}$$

where asterisk stands for complex conjugate. Equation (5) is the expression for the analytically-transformed model, which will be referred to as the analyticized Tauc-Lorentz model (TL-an). In the transformed model, TL parameter $\varepsilon_1(\infty)$ is no longer necessary and the complex dielectric constant is now self-consistent. Instead, new parameter a is introduced, therefore the total number of parameters has not changed with respect to TL. Even though in the above integration the weight function is nonzero only above E_g, the new function takes nonzero, positive values also below E_g, as required, due to the tail contribution of $[E'-(E+ia)]^{-1}$

functions centered at energies higher than E_g. From Eq. (5), the two components $\varepsilon_{1,TL\text{-}an}$ and $\varepsilon_{2,TL\text{-}an}$ can be obtained by calculating the real and imaginary parts, respectively, although the explicit expression specified in its real and imaginary parts turns less compact than Eq. (5). Many, if not all, software packages could work directly with this equation in complex numbers.

The new function is analytic on the real axis and in the upper complex half plane. The following points result in removable singularities: $b(E)=0$, $b(E)=\pm d$, $b(E)=\pm d^*$, and $b(E)=\pm E_g$, with $a>0$. From these, only $b(E)=-d$ and $b(E)=d^*$ are in the upper half plane. These, along with all the former ones, are removable singularities and the optical-constant function can be defined at each singularity.

$\mathrm{Log}(z)$ is a multivalued function. Here we choose its principal branch; hence, its argument is constrained within $(-\pi,\pi]$. Equation (5) presents branch cuts corresponding to the logarithm in the segments defined by two open intervals $(-\infty\text{-}ia,\text{-}E_g\text{-}ia)$ and $(E_g\text{-}ia,\infty\text{-}ia)$, symmetric with respect to the imaginary axis and placed in the lower half plane, and these intervals would move to the real axis for $a=0$; in other words, in the limit when $a=0$ the new function exactly reproduces the TL model, but it is precisely in this mathematical limit where the function is not analytic in the required domain. Regarding the logarithms where $b(E)$ is not present, their arguments are valued zero or a negative real number only if $C=0$, which would turn the TL model into a singularity peaked at E_0 (a Dirac delta), and this case can be considered outside TL model. Finally, it can be seen that expression (5) has the correct parity $\widetilde{\varepsilon}\left(-E^*\right)=\widetilde{\varepsilon}^*\left(E\right)$, a property naturally obtained here, whereas parity in TL model was forcedly introduced. The new model decays as E^{-2} (ε_1) and E^{-3} (ε_2) at large energies, which is fast enough to satisfy the requirements for KK analysis. Hence it satisfies all mathematical requirements for an analytic function and for KK analysis.

A further advantage of the new function given by Eq. (5) is that it is a single expression for $\widetilde{\varepsilon}$, so that all parameters of the model can be fitted with experimental data of either ε_1, ε_2, or both, whereas in TL model, $\varepsilon_1(\infty)$ is obtained only from ε_1 data and E_g is obtained basically from ε_2 data. Furthermore, $\widetilde{N}=n+ik$ can be obtained right away from Eq. (5) and hence all parameters of the model can be also fitted with experimental data of either n or k. Anyway, in the present model E_g parameter is more strongly dependent on either ε_2 or k than on their corresponding real parts.

3.2 Application of TL-an model to experimental data: SiC

In this sub-section we apply the new model to experimental data. Figure 1 compares experimental data of the dielectric constant of SiC films deposited by sputtering with fittings with TL and TL-an models. Self-consistent optical constants of SiC are taken from Larruquert *et al.* [12]. The two models were fitted separately in the spectral range 0.4 to 6.5 eV. Fitting parameters for both TL and TL-an models are given in table 1. In the linear plot of the dielectric constant, the two models seem to provide similar fittings. In the log-axis plot we see that TL model falls to zero at E_g=0.70 eV, differently to real data, whereas the TL-an model provides a better fit to ε_2 below E_g. Since the dielectric constant in the TL model was seen not to be analytic at E_g and smaller energies, it is not surprising that the main difference between TL and TL-an models is found precisely at E_g and at lower energies. TL-an model gives an overall good fitting, with a small discrepancy in the neighborhood of E_g. Such discrepancy could arise from uncertainty in the experimental data. Anyway, the present model, based on the model of Jellison and Modine and on Tauc's density of states, cannot address all the specific complexity that may be involved in a real material.

If the spectral range is extended to energies far smaller than the SiC bandgap, we get to its reststrahlen band. This feature is not included in either TL or TL-an models. Figure 2 displays the extended range that includes the reststrahlen band of SiC. We incorporated the

reststrahlen band in both models by adding a single Lorentz oscillator. This can be done by virtue of the linearity of the response to stimuli. The two added TL-an and Lorentz oscillator models are analytic and self-consistent, and so is the combined model. The fitting with TL plus the Lorentz oscillator is poor in the surroundings of the bandgap energy, whereas the fit with TL-an plus the Lorentz oscillator is remarkably good in the whole range. Best match was obtained by reducing *a* to 0.06 eV, leaving all other parameters as per Table 1.

Table 1. Fitting parameters for the TL and the TL-an models applied to SiC

Model	A(eV)	E_0 (eV)	C (eV)	E_g (eV)	$\varepsilon_1(\infty)$	*a* (eV)
TL	81.8	6.01	5.38	0.70	1.25	-
TL-an	87.2	6.07	5.56	0.72	-	0.09

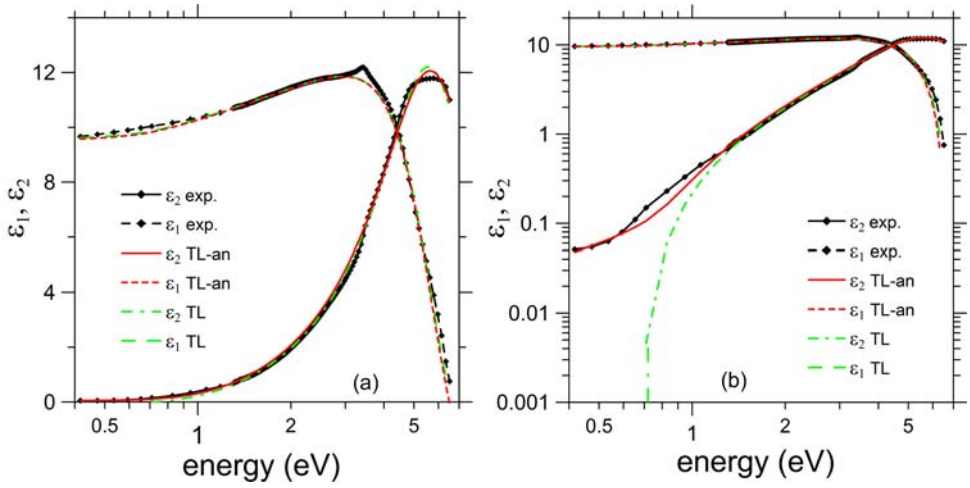

Fig. 1. Linear-axis (a) and log-axis (b) plot of the dielectric constant of thin films of SiC versus the logarithm of photon energy. Experimental data from Larruquert et al. [12] are compared with fittings with TL and TL-an models with parameters plotted in table 1

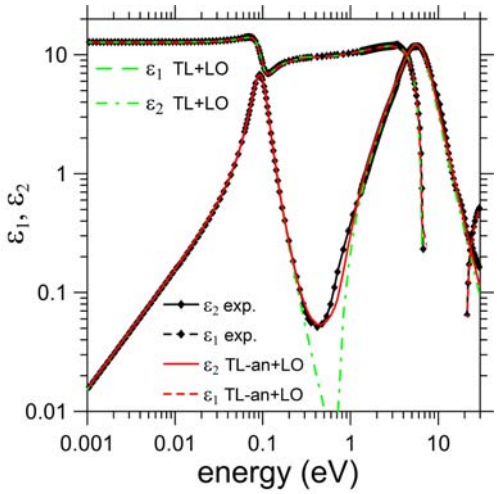

Fig. 2. Log-log plot of the dielectric constant of thin films of SiC versus photon energy extended to include the reststrahlen band. Experimental data from Larruquert et al. [12] are compared with fittings with TL and TL-an model using parameters plotted in table 1, except for the modification of *a* to 0.06 eV. The models were added a Lorentz oscillator to account for the reststrahlen band

The above extension of TL-an by adding a Lorentz oscillator can be generalized to the addition of as many Lorentz oscillators as necessary to model a specific material with many added features other than the basic TL shape behavior, which will be analytic due to the addition of only analytic terms.

3.3 Extension to include Urbach tail

The imaginary part of TL-an model progressively tends to zero below E_g, differently to the original TL model, where the function is zero for the whole energy range below the bandgap; this makes TL-an model more realistic than TL model, in addition to mathematically correct. However, the decay of ε_2 in TL-an model below E_g does not properly fit the materials with a so-called Urbach tail. For many semiconductors, as well as dielectric materials, the absorption coefficient $\alpha=4\pi k/\lambda$ often decays exponentially below E_g in what is called the Urbach tail:

$$\alpha(E)=\alpha_0 \exp\left(\frac{E}{E_0}\right) \tag{9}$$

This exponential decay is not properly fitted with TL-an model.

Foldyna *et al.* [6] modified TL model to incorporate Urbach tail. Foldyna's model, which will be referred to as TLU model, is expressed as a piecewise function with two functionalities in ε_2:

$$\varepsilon_{2,TLU}\left(E;A,E_0,E_g,C,E_c\right)=\frac{A_u}{E}\exp\left(\frac{E}{E_u}\right) \qquad E<E_c \tag{10a}$$

$$\varepsilon_{2,TLU}\left(E;A,E_0,E_g,C,E_c\right)=\frac{\left(E-E_g\right)^2 AE_0C}{\left(E^2-E_0^2\right)^2+C^2E^2}\cdot\frac{1}{E} \qquad E\geq E_c \tag{10b}$$

where E_c is the connection energy between the two functionalities; parameters E_u and A_u are chosen to assure continuity of both ε_2 and its first derivative at E_c, and they are explicitly shown by Foldyna et al. in [6]. TLU model is then given by a piecewise function, so that it is again non-analytic.

Though in Urbach tail it was the absorption coefficient α who had an exponential behaviour, Foldyna *et al.* [6] transferred this behaviour to ε_2, since *n* was considered by the authors as a constant over the Urbach tail fitting range.

TLU model involves several shortcomings common to TL model, except that ε_2 does not turn zero at energies below E_g:

a) TLU model is non-analytic at the connection energy between the two functionalities.

b) ε_2 is not an odd function in the exponential functionality, which adds to the parity problem in TL model.

c) In TLU model, ε_1 is obtained through KK integration of ε_2 but again needs the addition of a fitting parameter $\varepsilon_1(\infty)$.

Besides, TLU model adds a supplementary shortcoming: the model diverges at zero energy due to the term E^{-1}.

To solve all these problems, we derive a new function by applying the integral transformation given by Eq. (3a) to the following weight function:

$$\varepsilon_{2,U}\left(E;A,E_0,E_g,C,E_c\right)=EA_u\exp\left(\frac{E}{E_u}\right) \text{ at } E<E_c \tag{11a}$$

$$\varepsilon_{2,TL}\left(E;A,E_0,E_g,C,E_c\right)=\frac{\left(E-E_g\right)^2 AE_0C}{\left(E^2-E_0^2\right)^2+C^2E^2}\cdot\frac{1}{E} \text{ at } E\geq E_c \tag{11b}$$

where $\varepsilon_{2,U}$ stands for the imaginary part of the term with the Urbach tail. This new weight function is quite similar to the TLU model, but the present one presents a more realistic behaviour towards E=0. Thus, at energies close to E_g, the exponential term is dominant versus the energy factor in the denominator (Foldyna model) or numerator (present model); this energy factor plays a role at much smaller energies, where the function diverges in Foldyna model, and it plausibly tends to zero in the present model. Parameters E_u and A_u are selected to assure continuity of both the real weight function and its first derivative at E_c:

$$E_u = \frac{\left[E_c^{\,4} + \left(C^2 - 2E_0^{\,2}\right)E_c^{\,2} + E_0^{\,4}\right]\left(E_c - E_g\right)E_c}{-4E_c^{\,5} + 6E_g E_c^{\,4} + \left(4E_0^{\,2} - 2C^2\right)E_c^{\,3} + 4E_g\left(C^2 - 2E_0^{\,2}\right)E_c^{\,2} + 2E_g E_0^{\,4}} \tag{12}$$

$$A_u = \frac{AE_0C\left(E_c - E_g\right)^2 \exp\left(-\dfrac{E_c}{E_u}\right)}{\left[E_c^{\,4} + \left(C^2 - 2E_0^{\,2}\right)E_c^{\,2} + E_0^{\,4}\right]E_c^{\,2}} \tag{13}$$

The non-analytic model in Eq. (11) is now transformed to turn it into analytic in the same way that it was done with TL model. Hence we will integrate $[E'-(E+ia)]^{-1}$ functions with the Urbach tail term of Eq. (11a) in the range below E_c and with the TL term of Eq. (11b) above E_c. The analyticized model will be called TLU-an and it is obtained by the addition of the two mentioned terms:

$$\widetilde{\varepsilon}_{TLU-an}\left(E\right) = \widetilde{\varepsilon}_{U-an}\left(E; A, E_0, E_g, C, a, E_c\right) + \widetilde{\varepsilon}_{TL-an}\left(E; A, E_0, E_g, C, a, E_c\right) \tag{14}$$

Parameter E_c has been added to the list in the TL term, which is explained below. Hence the new model has six parameters to fit, the same number than Foldyna's model. The two terms of Eq. (14), which are obtained by applying Eq. (3a), are as follows:

$$\widetilde{\varepsilon}_{U-an}\left(E; A, E_0, E_g, C, a, E_c\right) = 1 + \frac{1}{\pi}\int_{-\infty}^{\infty}\frac{\varepsilon_{2,U}\left(E'\right)}{E' - E - ia}dE'$$

$$= \frac{A_u}{\pi}\left\{b\cdot\exp\left(\frac{b}{E_u}\right)\left[Ei\left(\frac{E_c - b}{E_u}\right) - Ei\left(\frac{-b}{E_u}\right)\right] + b\cdot\exp\left(\frac{-b}{E_u}\right)\left[Ei\left(\frac{b}{E_u}\right) - Ei\left(\frac{E_c + b}{E_u}\right)\right]\right.$$

$$\left. + 2\exp\left(\frac{E_c}{E_u}\right)E_u - 2E_u\right\} \tag{15}$$

where the sign of $\varepsilon_{2,U}$ in the integral of expression (15) was reversed for negative energies to turn it into an odd function.

$$\widetilde{\varepsilon}_{TL-an}\left(E; A, E_0, E_g, C, a, E_c\right) = 1 + \frac{AE_0C}{\pi}\left[\overline{F}\left(b, d, d^*\right) + \overline{F}\left(d, d^*, b\right) + \overline{F}\left(d^*, b, d\right)\right] \tag{16}$$

with:

$$\overline{F}\left(\alpha, \beta, \gamma\right) = \frac{\left(E_g + \alpha\right)^2 Log\left(E_c + \alpha\right) - \left(E_g - \alpha\right)^2 Log\left(E_c - \alpha\right)}{\alpha\left(\alpha^2 - \beta^2\right)\left(\alpha^2 - \gamma^2\right)} \tag{17}$$

The only difference between $\overline{F}$ of Eq. (17) and F of Eq. (6) is that in the former the new parameter E_c has been added, which replaces E_g in the argument of logarithms, so that $\overline{F}$ converges to F when E_c=E_g. Both $b(E)$ and d in Eqs. (15) to (17) are again given by Eqs. (7) and (8), respectively.

In the term $\widetilde{\varepsilon}_{U,an}$, Ei stands for the exponential integral [13,14]:

$$Ei(z) = -\int_{-z}^{\infty} \frac{e^{-t}}{t} dt \qquad |\arg(z)| < \pi \tag{18}$$

Function Ei(z) is included in mathematical packages for common-used computer softwares, such as Mathematica, MATLAB, and Maple. Discontinuities in the term $\widetilde{\varepsilon}_{TL,an}$ were commented in section 3.1; now, as E_g is replaced with E_c within the logarithms in Eq. (17), the singularities at $b(E)=\pm E_g$ shift to $b(E)=\pm E_c$ and they are again in the lower half plane; these singularities turn into removable when the $\widetilde{\varepsilon}_{U,an}$ term is added.

Eq. (15) is analytic in the upper half plane. $\widetilde{\varepsilon}_{U,an}$ presents branch cuts corresponding to the Ei functions in the segments defined by the open intervals(-∞-*ia*,0-*ia*) and (0-*ia*,∞-*ia*), both in the lower half plane. The function has isolated singularities at $b(E)=\pm E_c$ which counterbalance the singularities at the same energies of the $\widetilde{\varepsilon}_{TL,an}$ term, resulting in removable singularities. Singularities at $b(E)=0$ and at $b(E)=\infty$ are removable and are also in the lower half plane. At large energies $\widetilde{\varepsilon}_{U,an}$ asymptotically decays with E^{-2} in its real part and E^{-3} in its imaginary part.

Summarizing, TLU-an model is analytic: it has no pole either at the real axis or in the upper complex half plane. TLU-an is not a piecewise function; instead, it involves two terms, both defined in the whole spectrum, each one corresponding to one functionality of the original piecewise TLU model. Besides, $\widetilde{\varepsilon}_{TLU,an}$ has the correct parity, and the model does not diverge at zero energy as TLU does, due to the new functionality in Eq. (11a). Equation (14) provides the complex dielectric constant, which can be used to fit experimental data of either ε_2, ε_1 or both. Contrarily, either TL or TLU models specifically need data of ε_1 to fit parameter $\varepsilon_1(\infty)$. Anyway, as mentioned with the TL-an models, E_g parameter is more dependent on ε_2.

As for TL-an model, in TLU-an model $\widetilde{N} = n + ik$ can be immediately obtained from Eq. (15) and hence all parameters of the model can be also fitted with experimental data of either *n* or *k*, or both.

3.4 Application of analyticized TLU model to experimental data: Si_3N_4

Si_3N_4 is a material whose optical constants can be well described with a TL model and an Urbach tail. In Fig. 3, ε_2 experimental data are presented in the range 1-24 eV; data are taken from Philipp [15], and they are available in Palik's compilation [16]. Parameters of TLU-an model are displayed in Table 2 and they were fitted from ε_2 data, so that ε_1 was directly calculated here by taking the real part of the TLU-an model. The match between experimental data and the model is excellent. Notably, ε_2 tends to zero at zero energy, as expected for a semiconductor, contrarily to the divergence in Foldyna's model.

Table 2. Optimum parameters for TLU-an models applied to Si_3N_4

Model	A (eV)	E_0 (eV)	C (eV)	E_g (eV)	E_c (eV)	$\varepsilon_1(\infty)$	a (eV)
TLU-an	258.05	8.05	5.83	5.25	5.80	-	0.0002

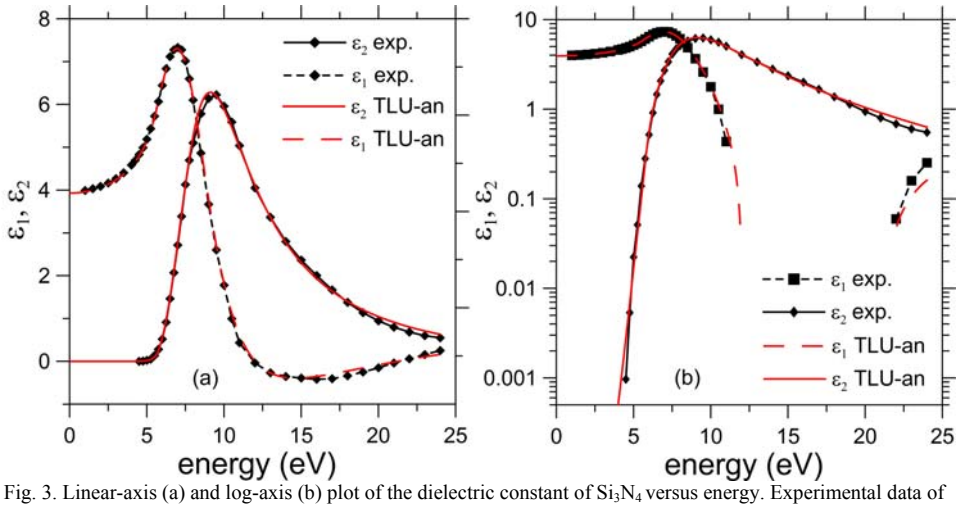

Fig. 3. Linear-axis (a) and log-axis (b) plot of the dielectric constant of Si_3N_4 versus energy. Experimental data of Philipp [15] are compared with a fitting of ε_2 with TLU-an model and with ε_1 obtained in the latter fitting using parameters plotted in table 2

4 Conclusions

It has been shown that TL model does not meet some requirements of optical constant functions, such as analyticity, and parity is artificially introduced. We have converted TL model into an analytic model TL-an based on the integration of $[E'-(E+ia)]^{-1}$ functions using the ε_2 expression of TL model as a weight function. TL-an is analytic and meets all the necessary mathematical requirements. The new model basically reproduces the TL model above the bandgap energy but it describes in a more realistic manner the behavior of the optical constants of amorphous semiconductors below the bandgap energy, where ε_2 non-physically cancels in TL model. Since the model is self-consistent, it allows obtaining both ε_2 and ε_1 even if only experimental data of ε_2 are available, whereas TL model needs both ε_2 and ε_1 data to obtain all parameters of the model. Both TL and TL-an models require 5 parameters to be fitted, where $\varepsilon_1(\infty)$ of TL model is replaced in the present model with a damping parameter. The new model was successfully applied to characterize the optical constants of SiC, both with the plain novel analytic model and also with the model combined with a Lorentz oscillator to include the reststrahlen band in the fitting.

The same procedure was also used to generate an analytic model, TLU-an, that also includes the Urbach tail; the procedure consisted in adding a weight function with an exponential term below the bandgap energy. In this model, ε_2 converges to zero at zero energy, as required. TLU-an model involves 6 parameters. The new model was successfully applied to characterize the optical constants of Si_3N_4, resulting in an excellent fit in a broad spectral range extending down to well below the bandgap energy. TLU-an results in a fully analytic model that enables optical-constant characterization in a wide spectrum including the specific TL spectral range and extending down to zero energy.

Funding

Spanish Programa Estatal de Investigación Científica y Técnica de Excelencia, Secretaría de Estado de Investigación, Desarrollo e Innovación, project number AYA2013-42590-P.